

# Fatigue behavior of rolled and forged tungsten at 25°, 280° and 480 °C



J. Habainy<sup>a</sup>, S. Iyengar<sup>a,\*</sup>, Y. Lee<sup>b</sup>, Y. Dai<sup>c</sup>

<sup>a</sup> Division of Materials Engineering, Lund University, Box 118, 22100 Lund, Sweden

<sup>b</sup> European Spallation Source ESS AB, Box 176, 22100, Lund Sweden

<sup>c</sup> Paul Scherrer Institute, Laboratory for Nuclear Materials, 5232 Villigen PSI, Switzerland

## HIGHLIGHTS

- Stress & strain-controlled fatigue tests on pure tungsten at 25°, 280° & 480 °C.
- Unirradiated, rolled and forged specimens in polished and unpolished condition.
- Min. tensile strength (MPa): 397 (25 °C), 472 (280 °C) and 363 (480 °C).
- Min. endurance limit (MPa): 137.5 (25 °C), 250 (280 °C) and 150 (480 °C).
- Marginal cyclic hardening observed at 480 °C.

## ARTICLE INFO

### Article history:

Received 17 March 2015

Received in revised form

12 June 2015

Accepted 14 June 2015

Available online 20 June 2015

### Keywords:

Fatigue properties

Tungsten target

Spallation source

## ABSTRACT

Pure tungsten has been chosen as the target material at the European Spallation Source facility in Lund. Calculations show that the target temperature can reach 500 °C momentarily during the spallation process, leading to thermal fatigue. Target life estimations require fatigue data at different temperatures and this work focuses on generating such data for pure, unirradiated, rolled and forged tungsten in the range 25°–480 °C.

For specimens oriented in the rolling direction, tensile tests at room temperature indicated Young's modulus values in the range 320–390 GPa, low levels of plasticity (<0.23%) and UTS values in the range 397 MPa (unpolished) and 705 MPa (Polished). UTS for forged specimens were around 500 MPa.

Stress-controlled fatigue tests were conducted in the tensile regime, with a runout limit of  $2 \times 10^6$  cycles. At 25 °C, unpolished specimens had fatigue limits of 150 MPa (rolling and transverse direction), and 175 MPa (forged). For polished specimens in the rolling direction, fatigue limits were higher at 237.5 MPa (25 °C) and 252.5 MPa (280 °C). The forged specimens showed slightly better fatigue properties and marginal cyclic hardening at 480 °C.

© 2015 Elsevier B.V. All rights reserved.

## 1. Introduction

Neutron scattering methods offer a powerful tool for characterizing materials and their behavior under controlled conditions. In this context, the need for a large scale neutron facility has led to the European Spallation Source which is currently under construction in Lund. In this facility [1], the neutrons are produced through a spallation process in tungsten which has a high neutron production density due to its high atomic number and density. The proton beam driving the spallation process is associated with energy and power levels of 2 GeV and 5 MW, respectively. The proton beam is pulsed at 14 Hz with a pulse duration of 2.86 ms and each beam pulse carries

357 kJ to the spallation volume. Beam pulses and beam trips during the operation introduce thermal fluctuations in the target, with temperatures reaching 775 K momentarily. Thermal fatigue is thus a distinct possibility and may cause target failure. In addition, the target is also subjected to high beam power as well as radiation damage. The life of the target is thus affected by a combination of these factors. In order to estimate the target life, it is essential to have reliable data on the mechanical properties of tungsten, both in the unirradiated and irradiated conditions. The following section presents a review of the studies on unirradiated tungsten.

### 1.1. Review of literature

Studies on tungsten have been mainly concerned with characterizing and improving its strength, ductility and fracture behavior

\* Corresponding author.

E-mail address: [srinivasan.iyengar@material.lth.se](mailto:srinivasan.iyengar@material.lth.se) (S. Iyengar).

at different temperatures. Tungsten is known to be brittle at ambient temperatures and exhibits ductility above the ductile to brittle transition temperature (DBTT). However, processing conditions affect DBTT and irradiation is also known to push it to higher temperatures.

Schmidt and Ogden [2] compiled data on the ultimate tensile strength (UTS), ductility, DBTT and other engineering properties of pure tungsten and its alloys, as a function of temperature. Foster and Stein [3] studied fully dense tungsten sheet specimens (0.5 mm thick) in bending at room temperature and reported a fatigue limit of 772 MPa under conditions of complete stress reversal and UTS values in the range 793–1630 MPa.

Beardmore and Hull [4] tested single crystals of tungsten in tension and observed ductility at low temperatures ( $-196^{\circ}$  to  $22^{\circ}$  °C), indicating that tungsten is extremely notch-sensitive and not necessarily inherently brittle. Discontinuous yielding was observed along [110], which may be attributed to the lower rate of dislocation multiplication in the vicinity of this direction [5].

Wronski and Chilton [6] did not observe any significant change in the tensile and compressive properties of polycrystalline cast tungsten due to pressurization at 1400 MPa. At  $420^{\circ}$  °C, they noted an elongation of 20% for tungsten, which became negligible at lower temperatures.

Braun and Sedlatschek [7] studied the effect of small alloying additions on the sintering, working and mechanical properties of tungsten. An addition of 0.01% thorium led to a 32% higher ductility, while chromium and vanadium additions showed the opposite effect. Raffo [8] studied the mechanical properties of vacuum arc-melted tungsten and tungsten–rhenium alloys in the temperature interval  $-196^{\circ}$  to  $537^{\circ}$  °C. Even at low concentrations (1 at%), Rhenium was effective in lowering the DBTT of tungsten, attributed to increased dislocation mobility.

Farrell et al. [9] observed that the DBTT in bending for tungsten sheets (wrought and powder metallurgical products) were the lowest at  $70^{\circ}$  °C. This increased to  $225^{\circ}$  °C after primary recrystallization at  $1150^{\circ}$  °C. DBTT after secondary recrystallization was in the range  $235^{\circ}$ – $280^{\circ}$  °C. Intergranular fracture was observed in specimens after primary recrystallization, which changed to transgranular cleavage after secondary recrystallization. In a following study [9], yield point inflections were noted during bending tests of sheet specimens above DBTT and the temperature dependence of yield and tensile strengths were similar. They observed a deviation from the classical Hall–Petch relationship and attributed it to the annealing treatment.

Forster and Gilbert [10] conducted 3-point bend tests on 99.9% pure tungsten wire specimens recrystallized at different temperatures to produce a range of grain structures. They found that fine-grained specimens had a lower DBTT ( $257$ – $307^{\circ}$  °C) relative to the coarse-grained specimens ( $297$ – $657^{\circ}$  °C). However, coarse grained materials withstand greater pre-yield strain before the initiation of fracture in the brittle regime.

Schmunk and Korth [11] studied tensile and low cycle fatigue properties of cross-rolled tungsten (DBTT  $\sim 300^{\circ}$  °C) at room temperature as well as at  $815^{\circ}$  °C. At both temperatures, a smaller strain interval was observed for recrystallized tungsten specimens compared to the as received material. Predictions from the universal slopes equation [12] were in agreement with fatigue data on the as received material at room temperature. At  $815^{\circ}$  °C, the average yield strength and UTS were 415 and 426 MPa respectively for the as received material, 115 and 240 MPa for recrystallized tungsten.

The dynamic recrystallization of potassium-doped tungsten during the rolling process was studied by Briant and Hall [13]. They observed high angle grain boundaries at low levels of deformation, with many dislocation-free grains and low angle grain boundaries

at higher levels of deformation. Annealing the rolled material in the temperature range  $1275^{\circ}$ – $1950^{\circ}$  °C showed abnormal grain growth, which emphasizes the need for close grain size control during the production of the target material.

Giannattasio and Roberts [14] investigated the strain-rate dependence of the brittle to ductile transition in single crystal and polycrystalline tungsten specimens. They found an Arrhenius relationship over a large strain rate interval, with an activation energy of 1.05 eV. As this value suggests double-kink formation on screw dislocations, the authors concluded that dislocation motion controls the transition.

Using micro hardness measurements, Zhang et al. [15] studied commercially pure ultrafine-grained tungsten and observed the DBTT to decrease from  $483^{\circ}$  to  $350^{\circ}$  °C as the grain size decreased from 10 to 0.9  $\mu$ m.

Rupp and Weygand [16] studied the fracture toughness of polycrystalline rolled tungsten in the brittle and semi-brittle regime, considering the crack orientation with respect to the rolling direction. With increase in temperature ( $-150^{\circ}$  to  $350^{\circ}$  °C), the fracture toughness improved for all types of specimens, with understandably better properties in the longitudinal direction. Fractographic studies showed that the longitudinal specimens were associated with transcrystalline cleavage at room temperature and intercrystalline failure at elevated temperatures. The authors have also developed a model which predicts the transition between the two fracture modes [17].

Using Auger electron spectroscopy and scanning electron microscopy, Gludovatz et al. [18] found that grain boundary impurities like phosphorus and oxygen did not affect the fracture behavior of tungsten materials. They concluded that factors such as size and shape of the grains, the extent of deformation and dislocation density have a greater impact on fracture.

Reiser et al. [19] carried out tensile tests on specimens made from commercially produced tungsten plates, rolled to 1 mm thickness. At room temperature, specimens oriented in the rolling direction and at  $45^{\circ}$  had high yield strengths (1350–1380 MPa) and surprisingly good ductility (1.5% strain in the rolling direction and 1% at  $45^{\circ}$ ), while the transverse specimens showed no ductility. The authors also reported isotropic behavior of the tungsten specimens at  $600^{\circ}$  °C and a tensile strength of about 700 MPa.

Yan et al. [20] investigated the effect of hot working and found that swaged and rolled tungsten had the highest relative density (99.1%) and a bending strength of 2180 MPa. They also noted that the properties could be improved by the addition of 1%  $\text{La}_2\text{O}_3$ .

Gaganidze et al. [21] studied the influence of anisotropic microstructure on the fracture behavior of polycrystalline tungsten up to  $1000^{\circ}$  °C. Intergranular fracture dominated in longitudinally oriented specimens up to  $600^{\circ}$  °C and transgranular cleavage in others at low temperatures.

Krsjak et al. [22] studied the fracture properties of rolled and hot isostatically pressed (HIP) tungsten and found that the DBTT for both materials were similar and in the range  $180^{\circ}$ – $230^{\circ}$  °C, while the flexural strength at room temperature was much higher for rolled tungsten (1050 MPa) than for the HIPed material (440 MPa).

Zhang et al. [23] determined the texture evolution during the rolling of tungsten. After annealing at  $1800^{\circ}$  °C for 2 h, full recrystallization was observed in 60% and 90% rolled tungsten. Goss and  $\theta$ -fiber textures were predominant in 80% rolled tungsten which was considered to have the best irradiation resistance.

Wurster et al. [24] reviewed the progress in the development of tungsten alloys for divertor structural and plasma facing materials. They have considered several approaches to increase ductility and fracture toughness as well as to decrease the DBTT by alloying additions and the use of fine-grained materials. The main challenge is in extending the excellent ductile properties of thin foils to bulk

materials and to ensure optimal irradiation resistance in the material.

## 1.2. Present work

Most of the studies on the mechanical properties of tungsten reviewed in the previous section used nearly fully dense, miniature sized or thin specimens. As tungsten has been found to be extremely notch sensitive, it is important to note the production method and specimen size while characterizing its mechanical properties. Further, fatigue data are very important in applications such as the design of the spallation target at ESS. However, published data on the fatigue behavior of pure bulk tungsten are limited to a few studies based on bend tests [3] and a low cycle fatigue study on cross-rolled tungsten subjected to fully reversible stresses [11]. Hence, the present study was taken up to obtain fatigue and tensile data for unirradiated, polycrystalline, bulk tungsten specimens obtained from powder metallurgical processing. Keeping in mind the temperatures relevant to the ESS project, tensile and fatigue tests on tungsten were carried out at 25°, 280° and 480 °C.

## 2. Materials and methods

Table 1 presents the impurity content of rolled and forged tungsten specimens used in this work. Most of the rolled specimens were oriented along the rolling direction, with a few oriented in the transverse direction. In order to determine the variation in fatigue strength due to surface quality, both unpolished and electropolished tungsten were tested. The specimen geometries used for room and high temperature tests are shown in Fig. 1. All the specimens were supplied by Beijing Tian-Long Tungsten & Molybdenum Co. and tested in the as received condition. The rolled high temperature samples were manufactured from a 20 mm thick sheet which had been rolled four times in the temperature interval 1500°–1650 °C, with a 20–25% reduction in each step. The smaller room temperature samples were machined from sheets rolled 5 times at a temperature of 1450°–1650 °C. The forged fatigue and tensile specimens were prepared from a tungsten plate hot forged in the temperature interval 1550°–1700 °C. This enabled a reduction in thickness from 150 mm to 90 mm achieved in a 3-step forging operation, during which the tungsten block was held in position on its sides under slight pressure.

In order to get an idea about the porosities in the samples, the densities were determined using the Archimedes principle. Mechanical testing was carried out using an MTS machine equipped with a Digital Electronic system supplied by Instron. For the high temperature tests, a furnace was installed and the grips were changed. The reported temperatures were measured at the surface of the specimen using a chromel–alumel (type K) thermocouple.

The tensile testing followed the standards set in ASTM E8/E8M [25], and the displacement rates were in the range of

0.6–2 mm·s<sup>−1</sup>. The stress-controlled fatigue testing was performed according to ASTM E739 [26] and only in the tensile regime. The minimum load was 0.1 kN and the load reversal frequency was in the interval 20–30 Hz. The up and down method [27,28] was used to determine the fatigue limits, with the runout condition set at  $2 \times 10^6$  cycles. Stress amplitudes employed in the fatigue testing were 100–350 MPa.

Strain controlled fatigue testing [29] was also performed to obtain the cyclic stress–strain curves and determine the degree of hardening of the materials. The tests were done using the Multiple Step Test method (MST) [30,31] with fully reversed strain cycles. At 280 °C the strain amplitude was initially set to 0.1% and increased in steps of 0.1% when saturation was observed. For the test at 480 °C, an amplitude sequence of 0.42, 0.58 and 0.75% was used. In both cases the strain rate was 2 mm s<sup>−1</sup>.

## 3. Physical properties

Six types of specimens were tested at three temperatures and each specimen was assigned an identification number based on the test temperature, the manufacturing method (F: Forged; R: Rolled), specimen orientation (L: Longitudinal – along the rolling direction; T: Transverse), and surface quality (P: Electropolished; U: Unpolished).

The results from the tensile and the fatigue tests, and metallographic examination are presented in the following sections.

### 3.1. Density

Densities of powder metallurgical products can vary significantly depending on the method of production and the densification treatments used. For pure tungsten at 20 °C, based on pycnometric measurements, the density has been reported as  $19.25 \pm 0.004$  Mg m<sup>−3</sup> [32]. This value is in excellent agreement with the theoretical density value calculated for the body-centered cubic form of tungsten using a lattice parameter value of 0.31652 nm reported in Ref. [33].

In this work, density measurements were carried out using a Mettler Toledo Precision Balance equipped with a Density Kit. For the rolled and forged specimens used in this study, the density values were determined to be 19.2303 and 18.8802 Mg m<sup>−3</sup> respectively. These values represent the average of three measurements with different samples at 23.1 °C. The corresponding porosities were estimated to be 0.1 and 1.92% respectively.

### 3.2. Hardness

Hardness measurements, both macro and micro, were carried out on room temperature specimens. Macrohardness tests were performed using a Sematic Durometer, and micro hardness tests using a Knoop diamond indenter mounted on a Leica DMRME light optical microscope. The average macrohardness was observed to be slightly above 40 HRC for all samples except for the forged unpolished ones (35.8 HRC). These have the lowest minimum value, the lowest average and the largest scatter, which could indicate relatively rough surfaces. The rolled, unpolished specimens oriented in the transverse direction were marginally harder than the rest. Micro hardness values for all the samples were in the range 460–583 KHN.

### 3.3. Surface examination

The surfaces of all the test pieces were examined in an optical microscope prior to testing. All of the surfaces were characterized by cracks, machining stripes and pores. The electropolished surfaces were slightly smoother, although there was a large variation

**Table 1**  
Impurity elements in tungsten.

Element	Max. content (in ppm)
O	50
Mo	30
Fe, C	10
Ca	8
As	7
Ni, Mg, Cr, Al	5
V, Sb, Ti, Mn, S, Co	4
Sn, Cu, Bi, Cd, Pb	1
Si	0.56
K	0.13

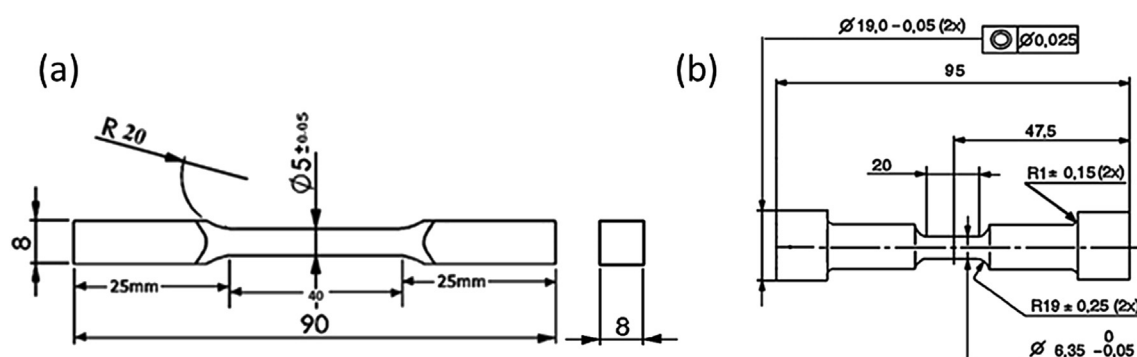


Fig. 1. (a) Room and (b) High temperature test specimens (dimensions in mm).

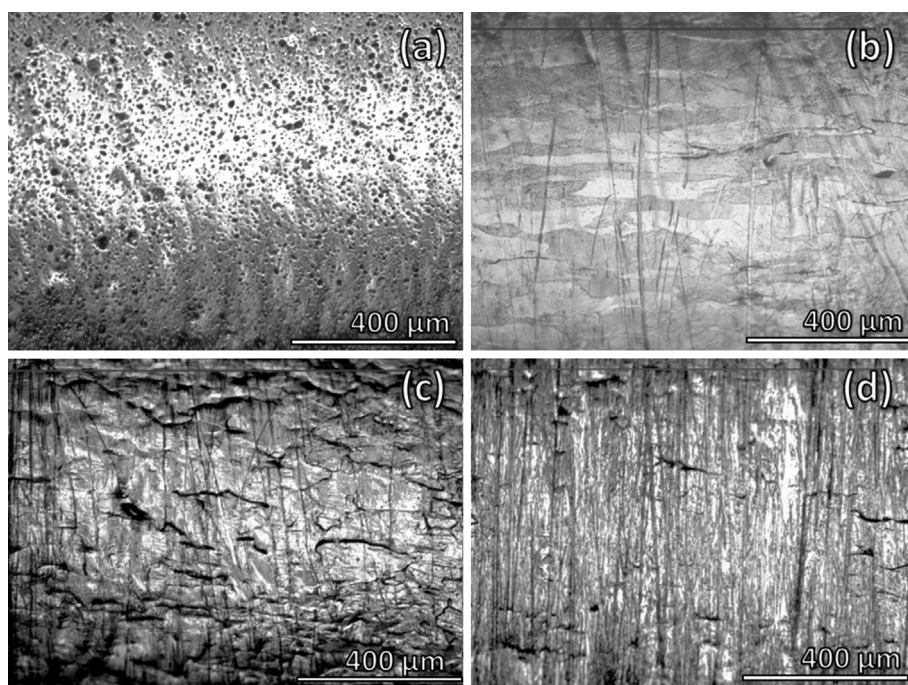


Fig. 2. Microscopic examination of the polished forged and rolled specimens before testing (a) HFP (b) RLP (c) RTP (d) HLP.

in the quality of polishing. The room temperature forged, unpolished specimens were associated with very rough surfaces with deep stripes and relatively large holes ( $>100 \mu\text{m}$  in diameter). The high temperature forged and polished pieces (HFP) had a relatively more even surface, but still contained plenty of pores (Fig. 2). The room temperature polished tungsten oriented in the rolling direction (RLP) proved to have the best surface finish. The grains were visible in these specimens, as shown in Fig. 2b. These elongated grains were approximately  $400 \mu\text{m} \times 100 \mu\text{m}$ . The surfaces of a high temperature rolled and polished oriented in the rolling direction (HLP) and a room temperature polished specimen oriented in the transverse direction (RTP) are also displayed in the figure. The latter showed relatively more longitudinal cracks.

## 4. Results and discussion

### 4.1. Tensile testing

Stress–strain curves from the tests performed in tension are shown in Figs. 3–5.7. Mean values of the Ultimate Tensile Strength

(UTS) for rolled and forged tungsten are summarized in Table 2.

As expected, the data from room temperature tests (Fig. 3) show the brittle nature of pure tungsten, with almost no ductility observed before failure. Rolled (7) and forged (4) specimens were tested at this temperature. The difference in tensile strength between forged specimens with polished and unpolished surfaces was not observed to be significant. A close examination of the sample surfaces showed that the specimens had roughly the same amount of pores, scratches and cracks, suggesting that the polishing was not performed satisfactorily. Mean values of UTS and Young's modulus for the forged material were found to be 510 MPa and 340 GPa respectively.

For the rolled specimens, specimen orientation appeared to be more important than the surface condition. However, polished specimens showed significantly better tensile behavior relative to the unpolished specimens. The mean UTS values were determined to be 673 MPa and 458 MPa in the rolling and transverse directions, respectively. The total strain at  $25^\circ\text{C}$  was observed to be in the range of 0.11–0.21%. In view of the large difference in UTS values for different orientations, rolled specimens with longitudinal



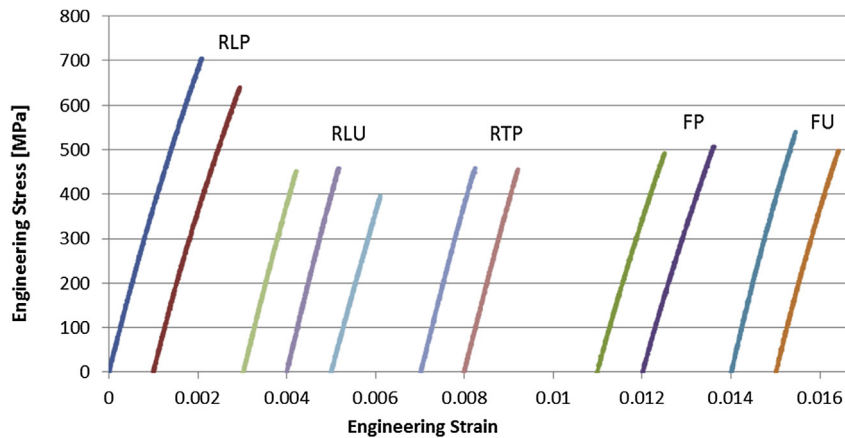


Fig. 3. Tensile data for rolled and forged specimens at 25 °C.

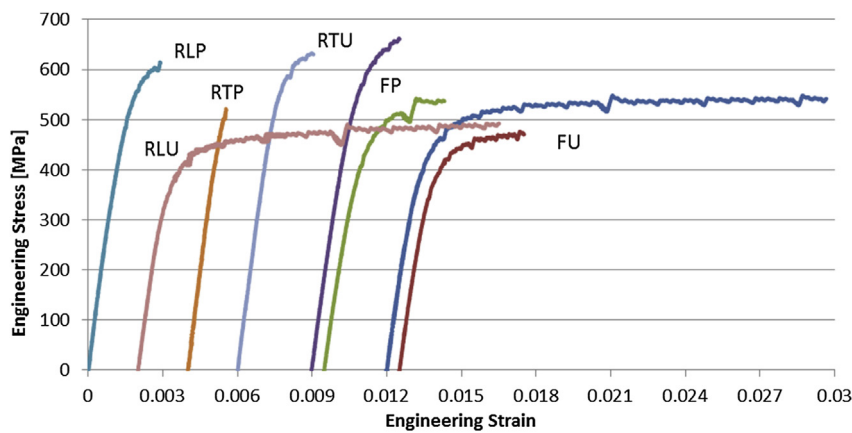


Fig. 4. Tensile data for rolled and forged tungsten at 280 °C.

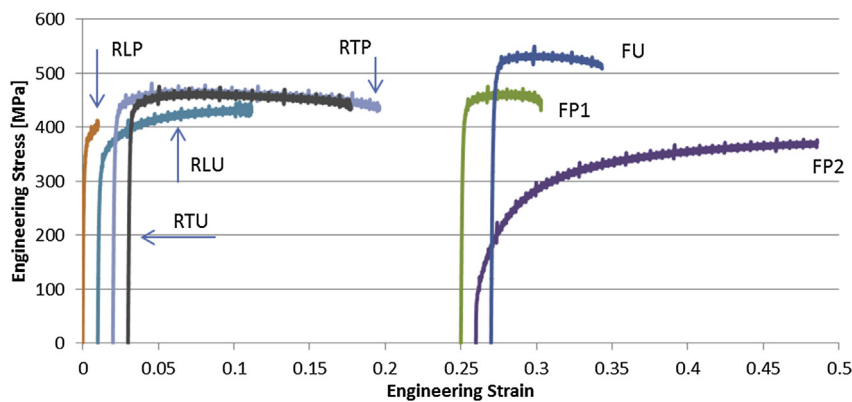


Fig. 5. Tensile data for rolled and forged tungsten at 480 °C.

orientation were chosen for fatigue testing. As the irradiated specimens are known to be very brittle, it was thought that testing of unirradiated specimens at room temperature would give some idea about the fatigue behavior of brittle tungsten with extremely low ductility.

At 280 °C (Fig. 4), a decrease in tensile strength and an increase in ductility were noted relative to those observed at room temperature. The total strain for the rolled specimens was in the range of 0.15–0.30%, as compared to 0.35–1.77% for the forged specimens which also showed a slight decrease in the UTS. The variation could

be due to the testing temperature being close to the DBTT for tungsten.

A substantial increase in ductility was observed at 480 °C (Fig. 5). One of the forged and polished specimens showed a total strain of over 25%. However, a second specimen of the same sort tested under the same conditions exhibited less ductility, indicating a variation in the quality of the specimens used. Fractographic studies (Fig. 6) showed cleavage fracture to a larger extent in the specimen with lower ductility.

Fig. 7 shows a comparison of the stress–strain curves for the

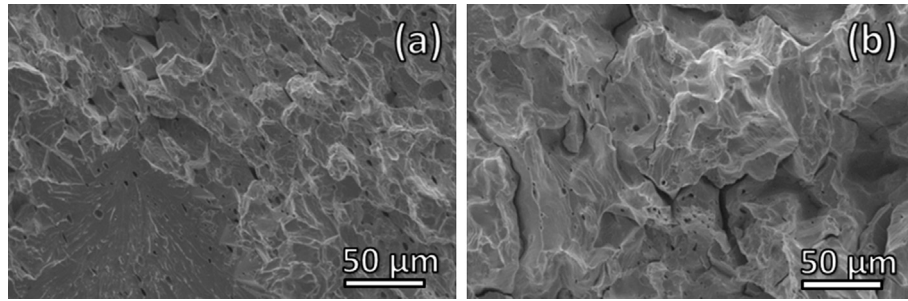


Fig. 6. Fracture surfaces of forged and polished tungsten specimens which failed at 480 °C. (a) & (b) correspond to FP1 and FP2 in Fig. 5.

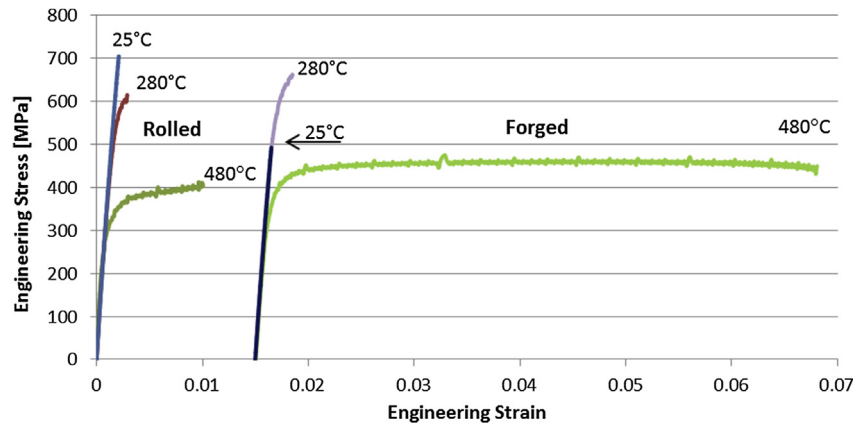


Fig. 7. Tensile data for polished rolled and forged tungsten at 25°, 280°, and 480 °C.

Table 2

Summary of UTS values obtained at different temperatures.

		Mean ultimate tensile strength [MPa]					
		25 °C		280 °C		480 °C	
		U	P	U	P	U	P
R	L	503 (397–571)	673 (640–705)	588 (495–681)	593 (571–615)	447	450
	T		458 (456–459)	633	522	475	481
F		519 (498–540)	500 (493–507)	507 (472–542)	540 (537–542)	550	525 (363–537)

polished specimens oriented in the rolling direction and the polished forged specimens, at three temperatures. At room temperature, the rolled specimen has a higher UTS value, but it is the other way around at 280 °C. However, the most noticeable difference is the total strain associated with forged tungsten.

The scatter in the results may be explained by the uneven surface for both the polished and unpolished specimens. A rough surface has a lot of stress concentration points where cracks can be initiated. Density variations in forged specimens could also contribute to the scatter in experimental data. For the rolled as well as forged material, Young's modulus data obtained from tensile tests were in the range 316–401 GPa. The effect of temperature was not significant in the range 25°–480 °C, but the forged material was

generally associated with a relatively lower stiffness. The UTS values obtained at different temperatures are shown in Table 2.

#### 4.2. Stress-controlled fatigue experiments

In the present study, fatigue data were obtained from a total of 12 different sets of stress-controlled experiments. More than 20 specimens were tested in some of the sets, while only a few were tested in others. While the minimum number of specimens required for different types of tests are specified by ASTM E739-10 [36], the number of specimens used in this work and the replication rates for the different sets of experiments are given in Table 3.

The results for sets with less than six specimens are considered

Table 3

Minimum number of specimens and replication rates in this study.

	25 °C						280 °C				480 °C	
	RLU	RLP	FU	FP	RTP	RTU	RLP	RLU	FP	FU	RLU	FP
No. of different stress levels	13	7	5	5	3	3	6	2	7	11	6	6
No. of tested specimens	22	16	12	12	3	3	9	2	9	12	6	9
Replication rate [%]	41	56	58	58	0	0	33	0	22	8	0	33

**Table 4**  
Endurance limits and maximum stress amplitudes at runout for rolled and forged tungsten specimens at different temperatures.

Stress amplitudes [MPa]				Endurance limit	No. of tests	Highest runout <sup>a</sup>
Sample						
25 °C	R	T	U	150.0	3	150.0
			P	137.5	3	137.0
		L	U	150.0	22	337.5
	P		237.5	16	300.0	
	F		U	175.0	9	200.0
		P	125.6	12	170.6	
280 °C		R	L	U	300.0	2
	P			252.5	12	290.0
	U			242.5	12	300.0
	F	P	212.5	9	250.0	
		U	150.0	6	150.0	
		P	175.0	9	187.5	

<sup>a</sup> Corresponds to  $2 \times 10^6$  cycles.

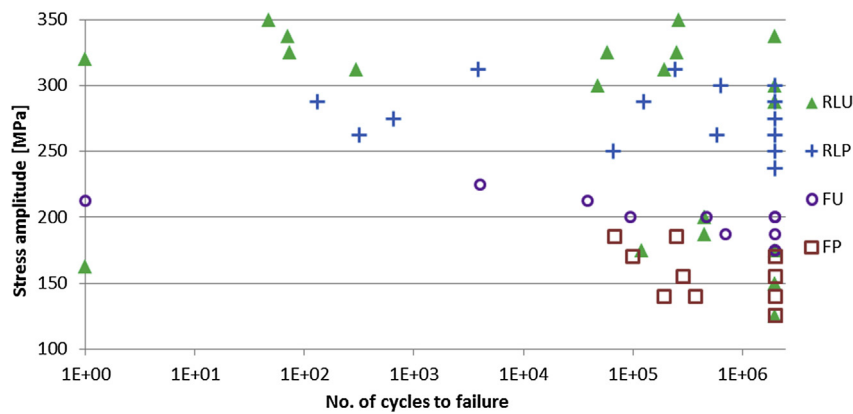


Fig. 8. Wöhler diagram for rolled and forged tungsten at 25 °C.

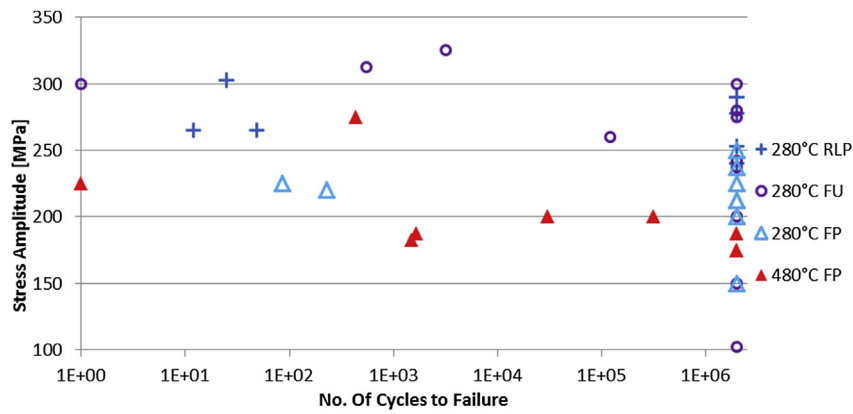


Fig. 9. Wöhler diagram for rolled and forged tungsten at 280° and 480 °C.

to be not statistically reliable and are not discussed further. The percent replication rate is good for most of the other sets except for FU at 280 °C, as well as RLU at 480 °C. However, the results give a good indication of fatigue behavior under these conditions. Table 4 presents a summary of the endurance limits obtained in this study. Wöhler diagrams corresponding to data obtained at the ambient and elevated temperatures are presented in Figs. 8 and 9.

At room temperature, there is a large variation in fatigue data for RLU. These specimens were associated with the highest runout stress (337.5 MPa), as well as one of the lowest endurance limits (150 MPa). The scatter for the polished counterpart was relatively

less and about half of the tested specimens failed at stress amplitudes between 237.5 and 312.5 MPa. Data for FU were lower relative to the RLP specimens, but more consistent. The 50% failure range for these specimens was within 25 MPa, as compared to 75 MPa for the RLP specimens. Somewhat unexpectedly, the endurance limit for FP (125.6 MPa) was the lowest, even lower than that of FU (175 MPa). This could be due to the fact that some of the FP test pieces fractured in the shoulder region having a radius of curvature, suggesting the presence of weak spots which originated probably during machining or electropolishing of the specimens.

At 280 °C the behavior of RLP and FU specimens were quite

similar and the endurance limits were determined to be 252.5 and 242.5 MPa respectively. At this temperature, the specimens generally performed the best and the experimental data showed limited scatter. At 480 °C, the endurance limit for FP (175 MPa) was observed to be 50 MPa higher than at room temperature.

It is quite difficult to predict the fatigue behavior of a material, if tests at a given stress amplitude can result in both immediate failure and runout. For example, such data were obtained for the FU specimens at 300 MPa and is typical even for the other types of test pieces. Instantaneous failures can be due to defective specimens with cracks on the surface or inside. This highlights the importance of proper surface treatment and good quality control. With brittle materials like tungsten, a certain amount of defects and scatter is inevitable. However, this should be kept to a minimum with the right manufacturing methods. A good example of the effect of polishing is seen in the case of rolled specimens at room temperature. The difference in the endurance limit between the polished and unpolished specimens is almost 90 MPa.

#### 4.3. Strain-controlled fatigue experiments

Strain-controlled fatigue tests were performed in order to understand the cyclic hardening behavior of pure tungsten. Assuming Ramberg–Osgood material behavior [34], the cyclic stress–strain curve is expressed as:

$$\varepsilon_a = (\sigma_a/E) + (\sigma_a/K')^{1/n'}$$

where  $\varepsilon_a$  is the strain amplitude,  $K'$  is the cyclic strength coefficient and  $n'$  is the cyclic strain hardening exponent. The method has been described in the introduction section.

Both rolled and forged tungsten exhibited virtually no plasticity at room temperature and it was not possible to evaluate the cyclic behavior from the data obtained. The specimen used at 280 °C was of RLU type. The initial strain level was set to 0.1% and increased in step of 0.1% when saturation was reached. Failure occurred after 22 cycles at the 4th level. From the stabilized hysteresis loop, the cyclic strength coefficient and the strain hardening exponent were determined as 1297 MPa and 0.108, respectively. A comparison between a monotonic tensile test of the same type of specimen and the stress levels of the hysteresis loop shows that the material undergoes marginal cyclic hardening. A forged and polished tungsten specimen showed a similar behavior at 480 °C. The strain levels used in this experiment were 0.42%, 0.58% and 0.75%. At the last level, the specimen only survived 9 cycles. The strength coefficient and the strain hardening exponent for this sample were

calculated to be 771 MPa and 0.09 respectively. Fig. 10 shows a comparison of hysteresis data from the strain-controlled fatigue test and a monotonic tensile test at 480 °C.

#### 4.4. Fractography

Fracture surfaces of 18 rolled as well as forged tungsten specimens in the polished as well as unpolished condition were studied in the scanning electron microscope after fatigue testing at various loads and temperatures. Fig. 11 presents fractographs for the rolled specimens. All these specimens failed in a brittle manner, more so at room temperature and show the characteristic chevron pattern with beach mark ridges.

The difference in fracture behavior between specimens oriented in the rolling and transverse directions is shown in Fig. 11(a) and (b). The test specimen oriented in the transverse direction shows a more brittle fracture with virtually no plasticity. Crack propagation is relatively easier in this specimen where cleavage fracture dominates. From Fig. 11(c), it is seen that the RLU specimen is associated with more ductility and some contribution from intergranular fracture. Fig. 11(d) shows that transgranular fracture dominates even at 280 °C, but displays some ductile areas and intergranular fracture. A feather pattern on a grain of tungsten is also clearly seen in this image.

The fracture surfaces of forged (unpolished) tungsten specimens which failed at 25° and 280 °C are shown in Fig. 12. Both the test pieces showed a number of pores, but exhibited different modes of brittle fracture. The grain sizes in the two specimens were observed to be dissimilar, with the high temperature specimen having smaller grains (~30 µm in diameter). It is interesting to see that some of the grains are completely detached, resembling loose gravel. This indicates a problem during sintering and the specimen failed soon after loading and did not show any sign of fatigue.

Fig. 13(a) and (b) show a comparison of the fracture surfaces of forged, unpolished samples at 25° and 480 °C. Both transgranular and intergranular fracture are observed in both cases, the former dominates at 25 °C. At the higher temperature, the fracture surface is characterized by a relatively smoother surface and deformation of the grains.

Fig. 13(c) and (d) compare the fracture surfaces of forged and rolled samples at 480 °C. The elongated grains are clearly seen in the rolled specimen and the fracture surface is showing a lot of deformation. Transgranular fracture can be clearly seen on the forged specimen surface, while delamination is observed in the rolled specimen. However, areas showing ductility and cleavage

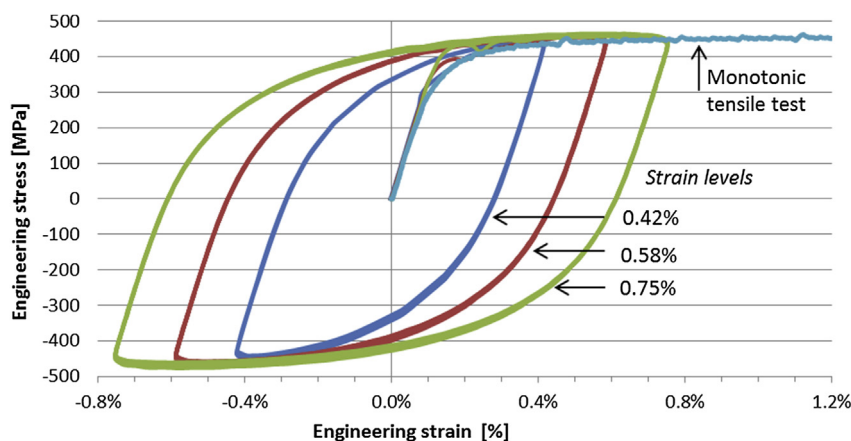
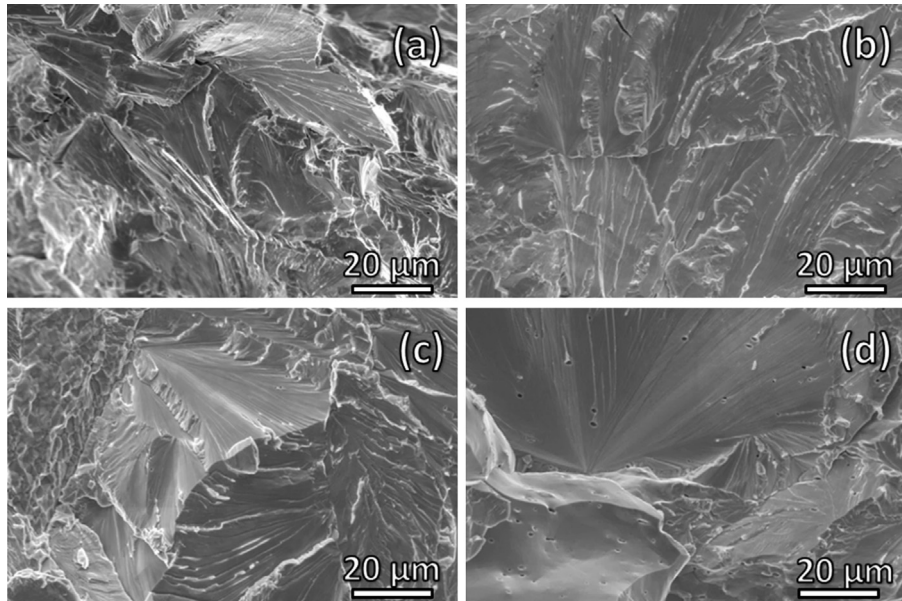
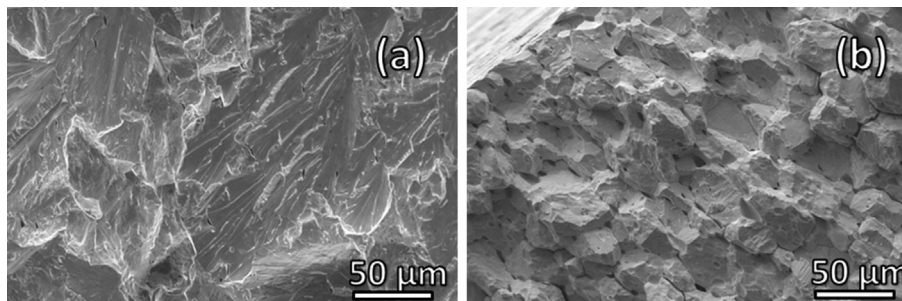


Fig. 10. Comparison between a strain controlled fatigue test and a monotonic tensile test of forged polished tungsten at 480 °C.





**Fig. 11.** Fracture surfaces of rolled specimens which failed after fatigue testing at different stress amplitudes and temperatures (a) RLP (25 °C, 175 MPa, 120841 cycles), (b) RTP (25 °C, 163 MPa, 136219 cycles), (c) RLU (25 °C, 200 MPa, 448951 cycles), (d) RLP (280 °C, 302.5 MPa, 25 cycles).



**Fig. 12.** Fracture surfaces of forged specimens after fatigue testing (a) FU 25 °C, 200 MPa, 473984 cycles; (b) FU 280 °C, 312.5 MPa, 545 cycles.

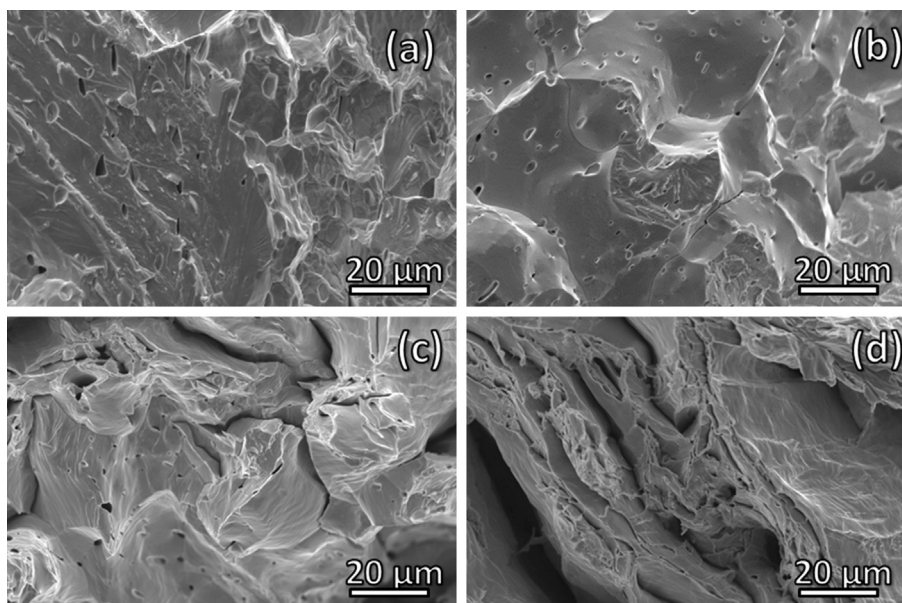


**Fig. 13.** Fracture surfaces of forged specimens at different temperatures and a rolled specimen which failed at 480 °C. (a) FP 25 °C, 156 MPa, 286335 cycles; (b) FP 280 °C, 220 MPa, 226 cycles; (c) FP 480 °C, 187.5 MPa, 1675 cycles; (d) RLU 480 °C, 250 MPa, 22392 cycles.

fracture can be seen in the case of the forged material.

## 5. Conclusions

Fatigue and tensile properties of forged and rolled tungsten have been studied at ambient and elevated temperatures. There is a wide scatter in data primarily due to the brittle nature of tungsten, but is also affected by the surface condition, volume fraction porosity, grain orientation, manufacturing method and specimen preparation. All the specimens showed brittle behavior at room temperature, with very little or no ductility. At 280 °C, most of the specimens were observed to be in the ductile regime, with improved fatigue properties. The rolled specimens showed relatively higher fatigue limits (237.5 MPa at 25 °C and 252.5 MPa at 280 °C for RLP specimens), higher density and slightly higher average hardness compared to the forged samples. In general, the specimens showed more ductility at 480 °C, with the strain controlled tests showing a marginal cyclic hardening effect.

In this work, UTS values obtained at room temperature varied from 397 to 705 MPa. Much higher UTS values of 793–1630 MPa have been reported by Foster and Stein [3]. In the same study, a fatigue limit of 772 MPa was determined from bending tests of very small samples (0.5 mm thick) at complete stress reversal. A 20% elongation was reported by Wronski and Chilton [6] for polycrystalline cast tungsten at 420 °C while Zhang et al. [15] reported a value of 1.5% at room temperature for specimens oriented in the rolling direction, as compared to values of 0.11–0.21% from this work.

In the present study, strain levels determined at 480 °C were in the range 1–17.6% for rolled specimens and 0.2–25% for the forged ones. These results are not easily compared with previous data due to differences in specimen size, sample preparation, production routes, and testing methods. The scarcity of fatigue data on pure tungsten is another issue. In the most relevant study to date, Schmunk et al. [11] conducted tensile and low-cycle fatigue tests on cross-rolled tungsten at room temperature and 815 °C. The fatigue experiments at the elevated temperature were run in fully reversed strain control. The room temperature specimens were run in load control at 1 Hz due to their brittleness. Two tests were terminated after 500,000 cycles without failure, corresponding to the stress ranges  $\pm 206.8$  and  $\pm 275.7$  MPa respectively. It may be noted that fatigue loading in the present study was in the tensile regime and the tests were terminated without failure only after  $2 \times 10^6$  cycles.

Even low levels of radiation damage can increase the DBTT for tungsten to >400 °C [35]. At 0.1 dpa, failure of tungsten in the brittle regime has been reported at 500 °C [36]. Data on the brittle behavior of unirradiated tungsten at low temperatures obtained in this study is therefore useful to the design of the ESS target wheel. However, much more work needs to be done in order to understand the behavior of tungsten during the operation of the target. Testing of irradiated samples is essential in this regard. In addition, attempts should be made to improve the quality of tungsten specimens and the test procedures to minimize the spread in experimental data.

## Acknowledgments

The authors are thankful to Zivorad Zivkovic, Sofie Borre, Andreas Löfberg and Kumar Babu Surreddi for invaluable assistance in the experimental work. Research funding and support from the European Spallation Source (ESS, Lund) is gratefully acknowledged.

## References

- [1] S. Peggs, ESS Conceptual Design Report, Feb 6, 2012. ISBN: 978-91-980173-0-4.
- [2] F.F. Schmidt, H.R. Ogden, Defence Metals Information Center Report no.191, Ohio, Columbus, September 27, 1963.
- [3] L.R. Foster, Jr, B.A. Stein, NASA Tech. Note D-1592, January 1963.
- [4] P. Beardmore, D. Hull, J. Less Common Met. 9 (1965) 168–180.
- [5] A.S. Argon, S.R. Maloof, Acta Met. 14 (1966) 1449–1462.
- [6] A.S. Wronski, A.C. Chilton, Scr. Met. 3 (1969) 395–400.
- [7] H. Braun, K. Sedlatschek, J. Less Common Met. 2 (1960) 277–291.
- [8] P.L. Raffo, J. Less Common Met. 17 (1969) 133–149.
- [9] K. Farrell, A.C. Schaffhauser, J.O. Stiegler, J. Less Common Met. 13 (1967), 141–155<sup>a</sup>, 548–558<sup>b</sup>.
- [10] R.H. Forster, A. Gilbert, J. Less Common Met. 20 (1970) 315–325.
- [11] R.E. Schmunk, G.E. Korth, J. Nucl. Mater. 103 & 104 (1981) 943–948.
- [12] S.S. Manson, Exper. Mech. 5 (1965) 193–226.
- [13] C.L. Briant, E.L. Hall, Met. Trans. A 20 (1989) 1669–1686.
- [14] A. Giannattasio, S.G. Roberts, Philos. Mag. 87 (2007) 2589–2598.
- [15] Y. Zhang, A.V. Ganev, J.T. Wang, J.Q. Liu, I.V. Alexandrov, J. Mater. Sci. Eng. A 503 (2009) 37–40.
- [16] D. Rupp, S.M. Weygand, J. Nucl. Mater. 386–388 (2009) 591–593.
- [17] D. Rupp, S.M. Weygand, Philos. Mag. 90 (2010) 4055–4069.
- [18] B. Gludovatz, S. Wurster, T. Weingärtner, A. Hoffman, R. Pippan, Phil. Mag. 91 (2011) 3006–3020.
- [19] J. Reiser, M. Rieth, B. Dafferner, S. Baumgärtner, R. Ziegler, A. Hoffman, Fusion Eng. Des. 86 (2011) 2949–2953.
- [20] Q. Yan, X. Zhang, T. Wang, C. Yang, C. Ge, J. Nucl. Mater. 442 (2013) S233–S236.
- [21] E. Gaganidze, D. Rupp, J. Aktaa, J. Nucl. Mater. 446 (2014) 240–245.
- [22] V. Krsjak, S.H. Wei, S. Antusch, Y. Dai, J. Nucl. Mater. 450 (2014) 81–87.
- [23] X. Zhang, Q. Yan, S. Lang, M. Xia, C. Ge, J. Nucl. Mater. (2015), <http://dx.doi.org/10.1016/j.jnucmat.2015.04.001>.
- [24] S. Wurster, N. Baluc, M. Battabyal, T. Crosby, J. Du, C. García-Rosales, A. Hasegawa, A. Hoffmann, A. Kimura, H. Kurishita, R.J. Kurtz, H. Li, S. Noh, J. Reiser, J. Riesch, M. Rieth, W. Setyawan, M. Walter, J.-H. You, R. Pippan, J. Nucl. Mater. 442 (2013) S181–S189.
- [25] ASTM E8/E8M-13a, Standard Test Methods for Tension Testing of Metallic Materials, ASTM International, West Conshohocken, PA, 2013. [www.astm.org](http://www.astm.org).
- [26] ASTM E739-10, Standard Practice for Statistical Analysis of Linear or Linearized Stress-life (S-N) and Strain-life ( $\epsilon$ -N) Fatigue Data, ASTM International, West Conshohocken, PA, 2010. [www.astm.org](http://www.astm.org).
- [27] R. Pollak, A. Palazotto, T. Nicholas, Mech. Mater. 38 (2006) 1170–1181.
- [28] S.-K. Lin, Y.-L. Lee, M.-W. Lu, Int. J. Fatigue 23 (2001) 75–83.
- [29] ASTM E606/E606M-12, Standard Test Method for Strain-controlled Fatigue Testing, ASTM International, West Conshohocken, PA, 2012. [www.astm.org](http://www.astm.org).
- [30] J. Polák, M. Hájek, Int. J. Fatigue 13 (1991) 216–222.
- [31] J. Polák, M. Klesnil, P. Lukáš, Mater. Sci. Eng. 28 (1977) 109–117.
- [32] E. Lassner, W.-D. Schubert, Tungsten – Properties, Chemistry, Technology of the Element, Alloys and Chemical Compounds, Kluwer Academic/Plenum, New York, 1999.
- [33] CRC Handbook of Chem. & Phys, 95<sup>th</sup> ed., 2014–2015 online, sec.12\_05\_86.
- [34] S. Suresh, Fatigue of Materials, second ed., 1998. Cambridge.
- [35] F. Ullmaier, F. Carsughi, Nucl. Instrum. Methods Phys. Res. B 101 (1995) 406–421.
- [36] I.V. Gorynin, V.A. Ignatov, V.V. Rybin, S.A. Fabrisiev, V.A. Kazakov, V.P. Chakin, V.A. Tsykanov, V.R. Barabash, Y.G. Prokofyev, J. Nucl. Mater. 191–194 (1992) 421–425.